

# Chapter 43

## The State-of-the-Art Numerical Tools for Modeling Landslide Tsunamis: A Short Review

Mohammad Heidarzadeh, Sebastian Krastel, and Ahmet C. Yalciner

**Abstract** We present a short review of the state-of-the-art numerical tools that have been used for modeling landslide-generated waves. A comparative study is conducted on the physical properties of earthquake- and landslide-generated waves suggesting that both dispersion and nonlinearity effects may be neglected for the former waves whereas they may be considered for the latter ones. We introduce landslide tsunami models and group them into three classes: (1) models treating the moving mass as a fluid, (2) models estimating the initial water surface, and (3) models fed by the transient seafloor deformation. Selection of a particular model from the list of models introduced here depends on: (1) the dimensions of the source, (2) the available computing capacities, (3) availability of fine bathymetric grid, and (4) the purposes of the modeling.

**Keywords** Submarine landslide • Landslide-generated waves • Tsunami • Numerical modeling

### 43.1 Introduction

Fifteen years after the 1998 Papua New Guinea (PNG) tsunami, a landslide tsunami triggered by a moderate earthquake ( $M_w$  7) claiming 2,200 lives (Synolakis et al. 2002), the potential hazard posed by submarine mass failures remains

---

M. Heidarzadeh (✉)

Cluster of Excellence “The Future Ocean”, Institute of Geosciences, Christian-Albrechts University zu Kiel, Kiel, Germany  
e-mail: [mheidarzadeh@geomar.de](mailto:mheidarzadeh@geomar.de)

S. Krastel

Institute of Geosciences, Christian-Albrechts-Universität University zu Kiel, Kiel, Germany

A.C. Yalciner

Department of Civil Engineering, Middle East Technical University, Ankara, Turkey

poorly understood at least in comparison to tectonic-generated tsunamis. Although scientists were surprised by the significant death toll following a moderate offshore earthquake on that tragic day, now they are well aware that landslide-generated waves pose a major risk to coastal communities since they may be triggered by moderate or small earthquakes and sometimes even aseismically.

The 1998 PNG event was a milestone in tsunami research, as it brought the attention of scientific community to the potential large tsunami hazards associated with submarine mass movements (Synolakis et al. 2002) though the phenomenon has been known long before the PNG event (e.g., Gutenberg 1939). In the aftermath of this catastrophe, the tsunami hazard of several locations in USA, Japan and other parts of the World were revisited by taking into account possible submarine mass failures. However, these efforts require new tools and techniques as the tsunami-genesis and hydrodynamics of landslide tsunamis differs from those of tectonic tsunamis, in several ways.

To address the increasing need for conducting tsunami hazard assessments from submarine landslides, here we review available numerical tools which have proven their capabilities in accurate modeling of landslide-generated waves.

## **43.2 Physical Differences of Landslide and Tectonic Tsunamis**

Table 43.1 compares the physical properties of landslides tsunamis with those of tectonic ones. The main differences are:

### ***43.2.1 Difference in Source Dimensions***

The seafloor deformation due to submarine tectonic displacements is normally of the order of hundreds of kilometers, whereas the dimensions of landslide sources are of the order of kilometers or less (Table 43.1). Therefore, tectonic tsunamis travel long distances with relatively little dispersion. Landslide-generated waves do not usually travel long distances due to their radial distribution of energy and their shorter wavelengths implying wave dispersion.

### ***43.2.2 Difference in Initial Seafloor Deformation***

Table 43.1 shows that the initial uplift or subsidence caused by submarine earthquakes is normally of the order of meters, but seafloor deformation due to landslides may be up to hundreds of meters. As a result of this relatively large seafloor

**Table 43.1** Comparing the physical properties of some landslide tsunamis with those of tectonic ones

Type	Event name	Type of tsunami source	L <sup>15</sup> (km)	W <sup>16</sup> (km)	SD <sup>17</sup> (m)	R <sup>18</sup> (m)	T <sup>19</sup> (min)	FFE <sup>20</sup>	SS <sup>21</sup> (m/s)	$\mu^{22}$	$\varepsilon^{23}$
Tectonic tsunamis	Dec. 26, 2004 (Indonesia) <sup>1</sup>	Earthquake ( <i>M<sub>w</sub></i> 9.1)	900	200	14	>40	40–120 <sup>11</sup>	Yes	4,000	0.002	$8 \times 10^{-6}$
	Mar. 11, 2011 (Japan) <sup>2</sup>	Earthquake ( <i>M<sub>w</sub></i> 9.0)	400	200	12	~40	40–100 <sup>12</sup>	Yes	4,000	0.005	$2 \times 10^{-5}$
	Feb. 27, 2010 (Chile) <sup>3,4</sup>	Earthquake ( <i>M<sub>w</sub></i> 8.8)	550	120	5	29	15–100 <sup>13</sup>	Yes	4,000	0.004	$5 \times 10^{-6}$
	July 12, 1993 (H-N-O) <sup>5</sup>	Earthquake ( <i>M<sub>w</sub></i> 7.8)	150	35	4.2	31.7	20–90 <sup>14</sup>	–	4,000	0.007	$2 \times 10^{-5}$
Landslide tsunamis	July 17, 1998 <sup>6</sup> (PNG)	Landslide after an earthquake ( <i>M<sub>w</sub></i> 7.0)	4.5	5	760	15	2–5	No	10–15	0.22	$2 \times 10^{-3}$
	Nov. 3, 1994 (Skagway) <sup>7</sup>	Construction works	0.33	0.16	15	9–11	1–3	No	35	0.1	$8 \times 10^{-3}$
	Nov. 18, 1929 (Grand Banks) <sup>8</sup>	Landslide after an earthquake ( <i>M<sub>w</sub></i> 7.2)	200	100	15	13	10–30	Yes	20	0.008	$3 \times 10^{-4}$
Mixed source	Dec. 30, 2002 (Stromboli) <sup>9</sup>	Landslide	2.2	0.7	30	11	0.5–1	No	30–60	0.5	$4 \times 10^{-3}$
	April 1, 1946 (Unimak) <sup>10</sup>	Both landslide and earthquake ( <i>M<sub>w</sub></i> 8.2)	–	–	–	42	–	Yes	–	–	–

<sup>1</sup>Fujii and Satake (2007), <sup>2</sup>Fujii et al. (2011), <sup>3</sup>Rabinovich et al. (2012), <sup>4</sup>Fritz et al. (2011), <sup>5</sup>Satake and Tanioka (1995), <sup>6</sup>Synolakis et al. (2002), <sup>7</sup>Rabinovich et al. (1999), <sup>8</sup>Fine et al. (2005), <sup>9</sup>Tinti et al. (2006), <sup>10</sup>Okal et al. (2003), <sup>11</sup>Rabinovich and Thomson (2007), <sup>12</sup>Heidarzadeh and Satake (2013), <sup>13</sup>Rabinovich et al. (2012), <sup>14</sup>Myres and Baptista (2001), <sup>15</sup>Length, <sup>16</sup>Width, <sup>17</sup>Seafloor deformation, <sup>18</sup>Maximum runup, <sup>19</sup>Period, <sup>20</sup>Far-Field effects, <sup>21</sup>Source speed, <sup>22</sup>Dispersion parameter, <sup>23</sup>Steepness parameter

deformation, landslides are capable of producing large runups in the near-field although their dimensions are usually small.

### ***43.2.3 Difference in Modeling Techniques***

Shallow water theory has been usually applied in the past decades for modeling of tsunamis which is based on the fact that tsunami wavelength ( $\lambda$ ) is much larger than the water depth ( $d$ ), or  $\mu = d/\lambda \ll 1$  (Table 43.1) where  $\mu$  is dispersion parameter. In fact, the effect of wave dispersion can be neglected for these long waves ( $\lambda/d > 20$ ) because the phase velocity of waves ( $c = \sqrt{gd}$ ) is a function of only water depth. However, landslide-generated waves are mostly classified as intermediate waves ( $2 < \lambda/d < 20$ ) or deep-water waves ( $\lambda/d < 2$ ). Due to the relatively small wavelengths of landslide-generated waves, dispersion plays a role in their propagation because the phase velocity of waves (e.g., for deep-water waves:  $c = \sqrt{\frac{g\lambda}{2\pi}}$ ) is a function of wavelength for this type of waves indicating that longer waves propagate faster than the shorter ones. Therefore, long-wave equations may be applied cautiously for modeling of landslide tsunamis or an alternative set of equations needs to be employed.

### ***43.2.4 Difference in Generation Mechanism***

As the speed of seismic waves responsible for seafloor deformation ( $\sim 4$  km/s) is much larger than the propagation speed of long water waves ( $\sim 0.1$ – $0.2$  km/s), it is often assumed that seafloor deformation due to a submarine earthquake occurs instantaneously. For landslides tsunamis, this is not a valid assumption because of the relatively lower speed of landslide movement on the seafloor ( $\sim 0.01$ – $0.1$  km/s, Table 43.1). This means that the relatively slow motion of landslides during the generation process of a tsunami needs to be taken into consideration.

### ***43.2.5 Linearity and Nonlinearity of the Waves***

In deep water, landslide tsunamis are most often linear and thus the steepness coefficient  $\varepsilon = a/\lambda$  is small (Table 43.1), where  $a$  is the wave amplitude. In shallow water, the waves become shorter and higher (steeper) until possible breaking. Here nonlinear models should be applied.

### ***43.2.6 Differences in Warning Systems and Tsunami Countermeasures***

The physical differences discussed between landslide and tectonic tsunamis necessitate different warning systems and tsunami countermeasures. While ground shaking and seismic records on seismometers provide useful warnings in many cases before the arrival of tectonic tsunamis, landslide tsunamis usually attack the coastal areas without warnings. As landslide tsunamis are normally characterized by extreme wave heights and are fairly unpredictable with regard to volume, location and release mechanism, construction of seawalls and other tsunami countermeasures may be less effective. Due to the unpredictability of landslide tsunamis, pre-computed landslide tsunami scenarios are not easily obtained for warning purposes whereas such pre-computed scenarios form the basis for tectonic tsunami warnings.

## **43.3 Modelling of Landslide Tsunamis**

Landslide-generated waves are usually dispersive, nonlinear, and their source speed is relatively slow. In fact, different methods for modeling landslide tsunamis are based on the way that we incorporate the aforesaid criteria into the modeling method. Among the main characteristics of the landslide-generated waves, possibly the slow movement of the source at the tsunami generation phase is the most important. Different numerical models used for landslide tsunami modeling can be identified by the way that they treat the tsunami generation phase. This is the basis for our classification of landslide tsunami models in the next section.

## **43.4 Available Numerical Models for Modelling Landslide Tsunamis**

In general, based on the way that a particular model treats the tsunami generation phase, we classify the landslide numerical models into three groups: (1) models that treat the submarine mass motion like the flow of a fluid with a particular density, (2) models that estimate the initial water surface using semi-empirical equations, and (3) models that are fed by the transient seafloor deformation at different times. Another classification was presented by Satake (2012). Table 43.2 presents a list of some numerical models that have been used for modeling of landslide-generated waves. Among the models presented in Table 43.2, some of them were originally developed for modeling of tectonic tsunamis which have been modified during the past decade to incorporate landslide sources (e.g., TUNAMI, and MOST). We briefly discuss below the classes of models.

**Table 43.2** Numerical models used for modeling of landslide-generated waves

Type	Name	Developer	L/NL <sup>1</sup>	D/ND <sup>2</sup>	C/UC <sup>13</sup>	Case studies
Treating submarine mass as a fluid	–	Heinrich (1992)	NL	ND	C	Caribbean Sea <sup>4</sup>
	–	Jiang and LeBlond (1992)	NL	ND	C	–
	TWO_LAYER	Imamura and Imteaz (1995)	NL	ND	C	Marmara Sea <sup>3</sup>
	–	Tinti et al. (1999)	NL	ND	C	Stromboli, Italy
	–	Thomson et al. (2001)	NL	ND	C	1994 Skagway
	–	Assier-Rzadkiewicz et al. (2000)	NL	ND	C	1979 Nice event
	–	Kawamata et al. (2005)	NL	ND	C	1741 Oshima-Oshima
Estimating the initial water surface	–	Harbitz (1992)	L	ND	UC	Grand Banks (1929)
	MOST	Titov and Synolakis (1998)	NL	ND	UC	1998 PNG <sup>6</sup> South California <sup>7</sup>
	TUNAMI	Goto et al. (1997)	NL	ND	UC	Off. Indonesia <sup>8</sup>
	GEOWAVE	Watts et al. (2003)	NL	D	UC	1998 PNG
	NAMI DANCE	Insel (2010)	NL	D	UC	1994 Skagway
	COULWAVE	Lynett and Liu (2002)	NL	D	UC	Marmara Sea <sup>9</sup>
	–	Weiss et al. (2006)	NL	D	UC	North Carolina <sup>15</sup>
Transient Seafloor models	COMCOT	Liu et al. (1998)	NL	WD <sup>10</sup>	C	Valdes slide, Chile <sup>14</sup>
	–	Satake (2001)	NL	ND	C	Mediterranean Sea <sup>11</sup>
	–	Lynett and Liu (2002)	NL	WD <sup>10</sup>	C	1741 Oshima-Oshima <sup>12</sup> Hawaii Island <sup>12</sup> 1998 PNG <sup>5</sup>

<sup>1</sup>Linear model/non-linear, <sup>2</sup>Dispersive/non-dispersive, <sup>3</sup>Yalciner et al. (2002), <sup>4</sup>Heinrich et al. (1999), <sup>5</sup>Lynett et al. (2003), <sup>6</sup>Synolakis et al. (2002), <sup>7</sup>Borrero et al. (2004), <sup>8</sup>Brune et al. (2010), <sup>9</sup>Insel (2010), <sup>10</sup>Weak dispersion effect is included in which numerical dispersion is applied to mimic physical dispersion, <sup>11</sup>Iglesias et al. (2012), <sup>12</sup>Satake (2001, 2012), <sup>13</sup>Coupled/un-coupled, <sup>14</sup>Weiss et al. (2013), <sup>15</sup>Geist et al. (2009)

#### 43.4.1 Models Treating the Submarine Mass Like a Fluid Flow

In this class of models, the movement of the submarine mass is treated like the flow of a fluid with the density of  $\rho_2$ . Therefore, two fluid layers with densities of  $\rho_1$  and  $\rho_2$  are modeled (Fig. 43.1). Long wave approximations are usually applied for

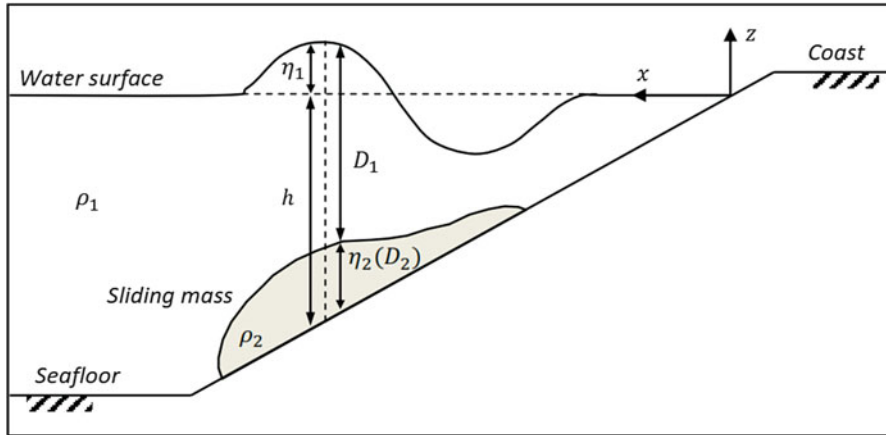


**Fig. 43.1** Sketch showing the principles of the landslide models that treat the moving mass like the flow of a fluid with density  $\rho_2$ . In this sketch,  $\rho_1$  and  $\eta_1$  represent the density and wave height of the ocean water and  $\eta_2$  is the thickness of the sliding mass

both the sliding mass and the resulting water waves. In this class of models, in some cases, only one flow with variable density in time and space is considered, e.g., the model by Heinrich (1992). For the simplest case in which the bottom friction and interfacial resistance are neglected, the 2D vertical (2DV) nonlinear long-wave equations (Imamura and Imteaz 1995) describing the system (Fig. 43.1) are:

For the water layer:

$$\frac{\partial(\eta_1 - \eta_2)}{\partial t} + \frac{\partial M_1}{\partial x} = 0 \tag{43.1}$$

$$\frac{\partial M_1}{\partial t} + \frac{\partial}{\partial x} \left( \frac{M_1^2}{D_1} \right) + gD_1 \frac{d\eta_1}{dx} = 0 \tag{43.2}$$

And for the sliding mass:

$$\frac{\partial \eta_2}{\partial t} + \frac{\partial M_2}{\partial x} = 0 \tag{43.3}$$

$$\frac{\partial M_2}{\partial t} + \frac{\partial}{\partial x} \left( \frac{M_2^2}{D_2} \right) + gD_2 \left( \alpha \frac{\partial D_1}{\partial x} + \frac{\partial \eta_2}{\partial x} - \frac{\partial h}{\partial x} \right) = 0 \tag{43.4}$$

in which  $g$  is the gravitational acceleration,  $M_1$  and  $M_2$  are flow discharges,  $\alpha$  is density ratio  $\left( \frac{\rho_1}{\rho_2} \right)$ , and other parameters are shown in Fig. 43.1.

The TWO\_LAYER model was successfully applied to the landslide sources in the Marmara Sea (Yalçımer et al. 2002). Other models of this class have been used for the modeling of the 1994 Skagway (Thomson et al. 2001) and the 1741 Oshima-Oshima (Kawamata et al. 2005) tsunamis (Table 43.2).

### 43.4.2 Models That Estimate the Initial Water Surface

Due to the complex nature of the generation phase of landslide tsunamis, some of the available numerical models simplify the generation phase by applying empirical equations. In fact, these models neglect the dynamic nature of the generation of waves by landslides. In this context, one set of empirical equations for modeling the generation phase of landslide tsunamis were proposed by Watts (1998) and described by Synolakis (2003). These authors estimated the 3D distribution of the initial sea level disturbance using 2DV numerical and experimental results. These empirical equations are based on a 2DV characteristic wave amplitude ( $\eta_{2d}$ ). According to Watts et al. (2005):

$$\eta_{2d} = 0.0286 T (1 - 0.75 \sin\theta) \left( \frac{b \sin\theta}{d} \right)^{1.25} \quad (43.5)$$

in which,  $T$  and  $b$  are the thickness and length of the sliding mass, respectively,  $d$  is the submergence depth, and  $\theta$  is the angle of the slope. Using Gaussian curve fits, Eq. (43.5) yields the 3D initial wave height of tsunami as follows (Synolakis 2003):

$$\eta_{3D}(x, y) = \frac{w}{\lambda + w} \sec^2 h^2 \left( \frac{3y}{w + \lambda} \right) \left[ -1.2 Z_{\min} \exp \left( - \left\{ 1.2 Z_{\min} \frac{x - X_{\min}}{\lambda Z_{\max}} \right\}^2 \right) + Z_{\max} \exp \left( - \left\{ \frac{x - X_{\min} - \Delta x}{\lambda} \right\}^2 \right) \right] \quad (43.6)$$

Here,  $Z_{\min}$  is the maximum depression of the water surface calculated using  $Z_{\min} = 2.1\eta_{2d}$ ,  $Z_{\max}$  is the maximum elevation obtained from  $Z_{\max} = 0.64 \eta_{2d} \left( 0.8 + \frac{0.2d}{b \sin\theta} \right)$ ,  $w$  is the width of the slide,  $\lambda$  is the characteristic wavelength given by  $\lambda = \frac{u_t}{a_0} \sqrt{gd}$ ,  $g$  is gravitational acceleration,  $u_t$  is the terminal velocity of slide, and  $a_0$  is the initial acceleration of slide.  $\Delta x$  is the distance between the crest of elevation wave and the trough of the depression wave, and given by  $\Delta x = 0.5 \lambda$ , and  $X_{\min}$  is the distance between the trough of the depression wave and the shoreline.

Figure 43.2 shows how a 3D initial wave of a landslide tsunami ( $\eta_{3D}$ ) is calculated from its characteristic wave height ( $\eta_{2D}$ ). To produce Fig. 43.2 (right panel), the characteristics of the 1998 PNG event were used for which the maximum elevation and depression in the initial profile of the water surface are 14 and 16 m, respectively. This class of landslide models is mostly composed of tectonic-tsunami models which have been modified to assign initial conditions using empirical equations.

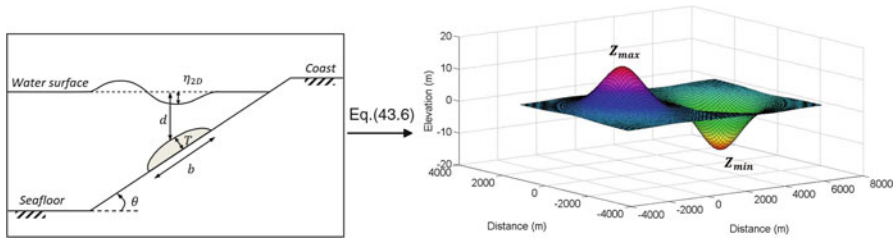


**Fig. 43.2** Sketch showing the principles of the landslide model that estimate the initial wave height generated by landslide sources. Left panel shows the parameters used for calculation of the characteristic wave height ( $\eta_{2D}$ ). Right panel shows the corresponding 3D initial wave height of tsunami ( $\eta_{3D}$ ) calculated using Eq. (43.6)

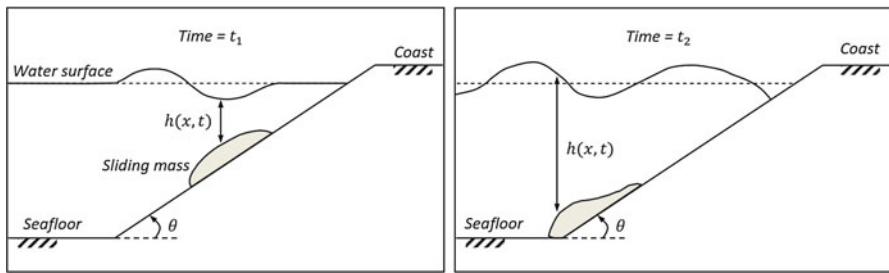


**Fig. 43.3** Sketch showing the principles of the landslide models that are inputted by the transient seafloor deformation at different times. This figure shows the seafloor states at two different times during the evolution of a submarine landslide

### 43.4.3 Models Fed by the Transient Seafloor Deformation

These models are based on the assimilation of the numerical scheme of the shape of the seafloor deformation at different times. As an example, Fig. 43.3 shows the seafloor states at two different times of  $t_1$  and  $t_2$  which can be used as inputs for the numerical simulations. In this case, the landslide source will be treated by implementing the forcing term of  $\frac{\partial h}{\partial t}$  in the continuity equation. By neglecting bottom friction and the Coriolis force, the nonlinear long-wave equations in a 2DV Cartesian domain take the following form (Wang 2009):

$$\frac{\partial \eta}{\partial t} + \frac{\partial M}{\partial x} = -\frac{\partial h}{\partial t} \tag{43.7}$$

$$\frac{\partial M}{\partial t} + \frac{\partial}{\partial x} \left( \frac{M^2}{h} \right) + gh \frac{\partial \eta}{\partial x} = 0 \tag{43.8}$$

in which the parameters are either as shown in Fig. 43.3 or were introduced above. The forcing term of  $\frac{\partial h}{\partial t}$  at the right side of the Eq. (43.7) represents the forcing from

the landslide source which can be calculated by differentiating the seafloor states that are inputted to the program at different times.

According to Table 43.2, the COMCOT model (Liu et al. 1998) has been recently used for landslide tsunami modeling in the Mediterranean Sea (Iglesias et al. 2012). Another such model was proposed by Liu et al. (2005).

## 43.5 Discussions and Conclusions

A range of landslide tsunami models have been discussed (Table 43.2). These models are either linear or nonlinear, dispersive or non-dispersive, and coupled or uncoupled. The most accurate models for landslide tsunami modeling are likely those which are nonlinear, dispersive and coupled. However, application of such sophisticated and computationally-costly models is reasonable only if enough information about seafloor bathymetry and sliding mass is available, and only if it is needed for a proper description of the physical processes involved. Among the models studied here, GEOWAVE (Watts et al. 2003) is fully nonlinear and dispersive. NAMI DANCE is also nonlinear and dispersion effect is included in one of its versions. Two other models, e.g., COMCOT and the model by Lynett and Liu (2002), are weakly dispersive by applying numerical dispersion. Most of the models in Table 43.2 are nonlinear and non-dispersive. Our short review suggests that the numerical tools used for landslide-generated waves are not, in general, as standardized as those used for tectonic tsunamis indicating that the recommendations by Synolakis et al. (2008) need to be applied for their standardization.

All of the models presented in Table 43.2 have proven their capabilities in varying degrees in modeling of landslide tsunamis, by reproducing observations from past events. Therefore, we cannot propose a particular model from our Table 43.2 for landslide tsunami hazard assessment as superior or more capable. Application of a particular model from Table 43.2 depends on several factors:

1. The dimensions of the source whether the dispersion can be neglected for the landslide source or not.
2. The available computing capacities: for example, dispersive models like the model by Liu et al. (2005) usually need relatively long CPU times.
3. Availability of fine bathymetric grid: most of the landslide tsunami models need relatively small grid size compared to tectonic models.
4. The purpose of the modeling and the level of desired accuracy. In most cases, the final tsunami runup height and arrival time to coastlines are the purposes of modeling. In many cases dispersion is important for the propagation phase. The wave length is important for amplification and run-up.

**Acknowledgments** This study was funded by the Alexander von Humboldt Foundation in Germany. The first author is grateful to Prof. Kenji Satake (University of Tokyo, Japan) for his

supports and fruitful discussions. This manuscript benefited from detailed and constructive reviews by Dr. Carl B. Harbitz (Norwegian Geotechnical Institute, Norway), Prof. Costas E. Synolakis (University of Southern California, USA) and Dr. Anawat Suppasri (Tohoku University, Japan) for which we are sincerely grateful.

## References

- Assier-Rzadkiewicz S, Heinrich P, Sabatier PC, Savoye B, Bourillet JF (2000) Numerical modeling of a landslide-generated tsunami: the 1979 Nice event. *Pure Appl Geophys* 157(10):1707–1727
- Borrero JC, Legg MR, Synolakis CE (2004) Tsunami sources in the southern California bight. *Geophys Res Lett* 31(13):L13211
- Brune S, Babeyko AY, Gaedicke C, Ladage S (2010) Hazard assessment of underwater landslide-generated tsunamis: a case study in the Padang region, Indonesia. *Nat Hazards* 53(2):205–218
- Fine IV, Rabinovich AB, Bornhold BD, Thomson RE (2005) The Grand Banks landslide-generated tsunami of November 18, 1929: preliminary analysis and numerical modeling. *Mar Geol* 215:45–57
- Fritz HM et al (2011) Field survey of the 27 February 2010 Chile tsunami. *Pure Appl Geophys* 168:1989–2010
- Fujii Y, Satake K (2007) Tsunami source of the 2004 Sumatra–Andaman earthquake inferred from tide Gauge and satellite data. *Bull Seismol Soc Am* 97(1A):S192–S207
- Fujii Y, Satake K, Sakai S, Shinohara M, Kanazawa T (2011) Tsunami source of the 2011 off the Pacific coast of Tohoku earthquake. *Earth Planets Space* 63:815–820
- Geist EL, Lynett PJ, Chaytor JD (2009) Hydrodynamic modeling of tsunamis from the Currituck landslide. *Mar Geol* 264(1):41–52
- Goto C, Ogawa Y, Shuto N, Imamura F (1997) Numerical method of tsunami simulation with the leap-frog scheme (IUGG/IOC time project), IOC Manual, UNESCO, No. 35
- Gutenberg B (1939) Tsunamis and earthquakes. *Bull Seismol Soc Am* 29(4):517–526
- Harbitz CB (1992) Model simulations of Tsunamis generated by the Storegga Slides. *Mar Geol* 105:1–21
- Heidarzadeh M, Satake K (2013) Waveform and spectral analyses of the 2011 Japan Tsunami records on Tide Gauge and DART stations across the Pacific Ocean. *Pure Appl Geophys* 170(6–8):1275–1293. doi:10.1007/s00024-012-0558-5
- Heinrich P (1992) Nonlinear water waves generated by submarine and aerial landslides. *J Waterw Port, Coast, Ocean Eng ASCE* 118(3):249–266
- Heinrich P, Guibourg S, Mangeney A, Roche R (1999) Numerical modeling of a landslide-generated tsunami following a potential explosion of the Montserrat volcano. *Phys Chem Earth A* 24(2):163–168
- Iglesias O, Lastras G, Canals M, Olabarrieta M, González M, Aniel-Quiroga Í, Otero L, Duran R, Amblas D, Casamor JL, Tahchi E, Tinti S, De Mol B (2012) The BIG’95 submarine landslide-generated tsunami: a numerical simulation. *J Geol* 120(1):31–48
- Imamura F, Imteaz MA (1995) Long waves in two layer, governing equations and numerical model. *Sci Tsunami Hazards* 13:3–24
- Insel I (2010) Landslide characteristics and tsunami generation, MSc thesis in METU Department of Civil Engineering, Coastal and Ocean Engineering Division
- Jiang L, LeBlond PH (1992) The coupling of a submarine slide and the surface waves which it generates. *J Geophys Res* 97(C8):12731–12744
- Kawamata K, Takaoka K, Ban K, Imamura F, Yamaki S, Kobayashi E (2005) Model of tsunami generation by collapse of volcanic eruption: The 1741 Oshima-Oshima tsunami. In: Satake K (ed) *Tsunamis*. Springer, Dordrecht, pp 79–96
- Liu PL-F, Woo S-B, Cho Y-S (1998) Computer programs for tsunami propagation and inundation. Technical report, Cornell University

- Liu PL-F, Wu T-R, Raichlen F, Synolakis C, Borrero JC (2005) Runup and rundown generated by three-dimensional sliding masses. *J Fluid Mech* 536:107–144
- Lynett P, Liu PL-F (2002) A numerical study of submarine–landslide–generated waves and run–up. *Proc R Soc Lond A* 458:2885–2910
- Lynett PJ, Borrero JC, Liu PL-F, Synolakis CE (2003) Field survey and numerical simulations: a review of the 1998 Papua New Guinea tsunami. *Pure Appl Geophys* 160:2119–2146
- Myres EP, Baptista AM (2001) Analysis of factors influencing simulations of the 1993 Hokkaido Nansei-Oki and 1964 Alaska tsunamis. *Nat Hazards* 23:1–28
- Okal EA, Plafker G, Synolakis CE, Borrero JC (2003) Near-field survey of the 1946 Aleutian tsunami on Unimak and Sanak Islands. *Bull Seismol Soc Am* 93(3):1226–1234
- Rabinovich AB, Thomson RE (2007) The 26 December 2004 Sumatra tsunami: analysis of Tide Gauge data from the World Ocean Part 1. Indian Ocean and South Africa. *Pure Appl Geophys* 164:261–308
- Rabinovich AB, Thomson RE, Kulikov EA, Bornhold BD, Fine IV (1999) The landslide-generated tsunami of November 3, 1994 in Skagway Harbor, Alaska: a case study. *Geophys Res Lett* 26(19):3009–3012
- Rabinovich AB, Thomson RE, Fine IV (2012) The 2010 Chilean tsunami off the west coast of Canada and the northwest coast of the United States. *Pure Appl Geophys*. doi:[10.1007/s00024-012-0541-1](https://doi.org/10.1007/s00024-012-0541-1)
- Satake K (2001) Tsunami modeling from submarine landslides. In: *Proceedings of the international Tsunami symposium, Seattle, Washington (USA), 7–10 August 2001, vol 6, paper 6–4*
- Satake K (2012) Tsunamis generated by submarine landslides. *Submarine mass movements and their consequences*, Springer, pp 475–484
- Satake K, Tanioka Y (1995) Tsunami generation of the 1993 Hokkaido Nansei-Oki earthquake. *Pure Appl Geophys* 144(3/4):803–821
- Synolakis CE (2003) Tsunami and seiche. In: Chen WF, Scawthorn C (eds) *Earthquake engineering handbook*. CRC Press, Boca Raton, pp 1–90, Chapter 9
- Synolakis CE, Bardet J-P, Borrero JC, Davies HL, Okal EA, Silver EA, Sweet S, Tappin DR (2002) The slump origin of the 1998 Papua New Guinea tsunami. *Proc R Soc Lond A* 458:763–789
- Synolakis C, Bernard E, Titov V, Kanoglu U, Gonzalez F (2008) Validation and verification of tsunami numerical models. *Pure Appl Geophys* 165(11–12):2197–2228
- Thomson RE, Rabinovich AB, Kulikov EA, Fine IV, Bornhold BB (2001) On numerical simulation of the landslide-generated tsunami of November 3, 1994 in Skagway Harbor, Alaska. In: Hebenstrait GT (ed) *Tsunami research at the end of a critical decade, vol 18, Advances in natural and technological hazards research*. Kluwer Academic Publishers, Dordrecht, pp 243–282, 304 p
- Tinti S, Bertolucci E, Romagnoli R (1999) Modeling a possible Holocene landslide-induced tsunami at Stromboli volcano. *Phys Chem Earth* 24(5):423–429
- Tinti S, Maramai A, Armigliato A, Graziani L, Manucci A, Pagnoni G, Zaniboni F (2006) Observations of physical effects from tsunamis of December 30, 2002 at Stromboli volcano, southern Italy. *Bull Volcano* 68(5):450–461
- Titov VV, Synolakis CE (1998) Numerical modeling of tidal wave runup. *J Waterw Port Coast Ocean Eng* 124(4):157–171
- Wang X (2009) *User manual for COMCOT version 1.7 (first draft)*, Cornell University, pp 65
- Watts P (1998) Wavemaker curves for tsunamis generated by underwater landslides. *J Waterw Port Coast Ocean Eng* 124(3):127–137
- Watts P, Grilli ST, Kirby JT, Fryer GJ, Tappin DR (2003) Landslide tsunami case studies using a Boussinesq model and a fully nonlinear tsunami generation model. *Nat Hazards Earth Syst Sci* 3(5):391–402
- Watts P, Grilli ST, Tappin D, Fryer GJ (2005) Tsunami generation by submarine mass failure. II: predictive equations and case studies. *J Waterw Port Coast Ocean Eng* 131(6):298–310

- Weiss R, Wunnemann K, Bahlburg H (2006) Numerical modelling of generation, propagation and run-up of tsunamis caused by oceanic impacts: model strategy and technical solutions. *Geophys J Int* 167:77–88
- Weiss R, Krastel S, Anasetti A, Wunnemann K (2013) Constraining the characteristics of tsunami waves from deformable submarine landslides. *Geophys J Int*. doi:10.1093/gji/ggt094. <http://gji.oxfordjournals.org/content/early/2013/04/05/gji.ggt094>
- Yalçiner AC, Alpar B, Altınok Y, Özbay İ, Imamura F (2002) Tsunamis in the Sea of Marmara: historical documents for the past, models for the future. *Mar Geol* 190(1):445–463